Desalination and Water Treatment
www.deswater.com
doi: 10.5004/dwt.2018.22827

130 (2018) 243–249
October

Removal of tetracycline antibiotic using cerium oxide nanoparticles and determination by HPLC

Behrooz Zargar*, Nahid Pourreza, Mahsa Samadifar

Department of Chemistry, Faculty of Sciences, Shahid Chamran University of Ahvaz, Ahvaz, Iran,
emails: zargar_b@scu.ac.ir (B. Zargar), npourreza@scu.ac.ir (N. Pourreza), samadi1371mahsa@gmail.com (M. Samadifar)

Received 14 November 2017; Accepted 24 July 2018

ABSTRACT

The presence of antibiotics in the environment threatens the health of humans and animals, seriously. In this respect, this study applies cerium oxide nanoparticles (CeO_2 NPs) as an adsorbent to remove tetracycline (TC) from aqueous solutions and investigates the effects of various parameters on the adsorption reaction. The studied parameters include pH, electrolyte concentration, TC concentration, amount of the adsorbent, flow rate of the solution, and the presence of several coexisting ions. According to the obtained results, the CeO_2 NPs are quite efficient for removal of TC at room temperature. Furthermore, adsorption of TC onto the CeO_2 NPs is fast and the corresponding isotherms fit the Langmuir model, perfectly. The proposed adsorption method is successfully employed to remove TC from various aqueous solutions including surface and drinking water samples.

Keywords: Tetracycline, Cerium oxide nanoparticles, HPLC; Removal

1. Introduction

Tetracycline (TC; $C_{22}H_{24}N_2O_8$) is one of the antibiotics that is widely used for treatment of humans and animals [1–3]. While some antibiotics can affect: just a specific type of bacteria (such as gram-positive or gram-negative bacteria), TC can treat a wide spectrum of bacteria (both gram-positive and gram-negative) [4]. Along with 30%–80% of antibiotics, TC can diffuse into the environment through various sources without any changes in its chemical structure [5,6]. It is while the presence of antibiotics in the environment can increase the resistance of pathogens against antibiotics and, therefore, threaten the ecosystem and human health [2]. For this reason, developing a quick and easy method to remove small amounts of antibiotics from surface water and biological samples is of great importance. In the case of TC, a variety of techniques, such as ozonation [7], electrocatalytic oxidation [8], photocatalytic degradation [9], sonochemical processing [10], biodegradation [11], and adsorption [2,12–15], have been reported. Particularly, adsorption has attracted the interest of many researchers. So that, carbon nanoparticles (NPs) [16], Fe-Mn binary oxide NPs [2], biochars [17], struvite [18], sulfur-doped manganese oxide [19], aluminum oxide [20], iron [21], vermiculite [22], and kaolinite [23] have been applied to adsorb TC and remove it from aqueous solutions.

A potential adsorbent for removal of TC is the NPs of cerium oxide (CeO_2) is the most commonly used metal oxide for industrial applications including catalysts, polishing materials, electrolyte materials of fuel cells, gas sensors, absorption, and luminescence. The advantages of CeO_2 NPs are low cost and high stability. In addition; CeO_2 NPs are harmless for the environment and have anticancer properties [24,25]. These properties of CeO_2 NPs have motivated their application for removal of arsenic and fluoride from surface water [26,27] and represent them as a potential adsorbent for removal of environmental contaminants. According to the importance of TC removal from water resources and the effectiveness of the adsorption method, this study employs this technique to remove the TC antibiotic from surface waters. In this respect, the TC content of the examined water is measured before and after adsorption onto CeO_2 NPs

* Corresponding author.

using high-performance liquid chromatography (HPLC). Based on the results, the CeO_2 NPs have a greater capacity and efficiency (93.8%) of TC removal from aqueous solutions, compared with the other adsorbents that have been adopted to remove TC (Table 1) [2,16–23].

2. Experimental

2.1. Chemicals and reagents

Almost all utilized materials were of analytical grade. Acetonitrile, water (HPLC grade) and TC were purchased from Merck (Darmstadt, Germany). The stock solution of TC (1,000 μg mL^{-1}) was prepared weekly by dissolving 0.01 g TC in methanol and diluting the solution in a 10 mL volumetric flask. The stock solution was kept in a dark place and below 4°C. The diluted solutions were prepared by diluting the stock solution with distilled water. Fig. 1 shows the chemical structure of TC hydrochloride.

2.2. Apparatus

The HPLC instrument (2500 model, Knauer, Germany) that was used to determine TC concentration was equipped with a 5000 model pump and a UV detector. pH of the solutions was measured by a pH-meter (model 623, Metrohm, Switzerland).

2.3. Chromatographic analysis

The stationary phase of the HPLC instrument was a C_{18} column with the 4.6 × 150 mm dimension and the mobile phase was a mixture of acetonitrile and 0.005 M oxalic acid at pH 3 (20:80 V/V). The flow rate was 1 mL min^{-1}. An injector valve with a 20 μL sampling loop was used for injection of the samples solutions into the HPLC instrument. The temperature of the column was set to 30°C. The spectrophotometric measurements were performed at 360 nm. To relate the measured absorbance intensities to a definite TC concentration, a linear calibration curve was obtained over the TC concentration range of 0.1–10 mg L^{-1} with an excellent correlation coefficient (R = 0.9988). The retention time of the TC peak at the applied chromatographic conditions was about 4 min.

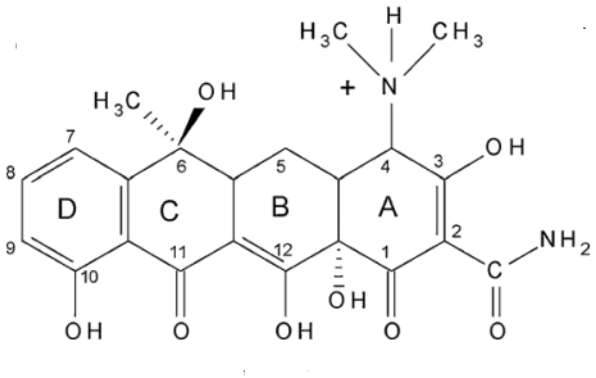

Fig. 1. Chemical structure of tetracycline.

2.4. General adsorption procedure

In a 25 mL volumetric flask, 125 μL of the stock solution (100 μg mL^{-1}) was added and the solution was brought to the specified volume with distilled water. 10 mg of the CeO_2 adsorbent was weighted and loaded in an extraction column with 10 cm length, after that the prepared TC solution was passed through the column using a vacuum pump with the 1.3 mL min^{-1} flow rate. Finally, 20 μL of the output solution was injected into the HPLC system and the removal percentage of TC was calculated. Fig. 2 shows a typical chromatogram of TC before and after the removal process.

3. Results and discussion

3.1. Characterization of the CeO_2 nanoparticles

Fig. 3 shows the TEM image of the CeO_2 NPs. According to this figure, the NPs are spherical in morphology and their average size is about 5–10 nm. Due to the random accumulation of the NPs, they seem to have a mesoporous structure [28]. The zero-charge point (PZC) of the CeO_2 NPs was measured by adding 0.05 g solid CeO_2 to 25 mL aqueous NaCl (0.1 M). Then, the pH of the suspension was adjusted on 3–10 by adding small volumes of 0.1 M HCl or NaOH and the resultant solution was stirred for 24 h. Based on Fig. 4, the PZC of the CeO_2 NPs refers to pH 8.

Table 1
Compilation of adsorption experiments for removal of tetracyclines using different materials and our research

Material	TCs adsorbed (mg g^{-1})	Removal%	References
Activated carbon NPs	1.90	74–88	[16]
Fe-Mn binary oxide	–	90	[2]
Biochars	58.80	70	[17]
Struvite	0.04	22	[18]
Sulfur-doped manganese oxide	203	86.4	[19]
Aluminum oxide	–	43	[20]
Iron	24	–	[21]
Vermiculite	36.80	–	[22]
Kaolinite	47	–	[23]
Cerium oxide NPs	79.36	93.8	Our study

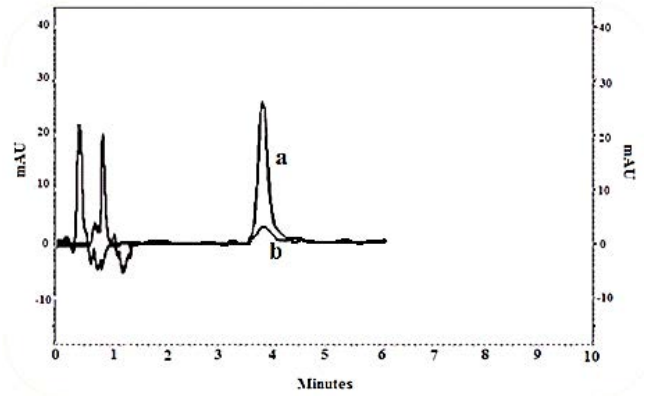

Fig. 2. Chromatogram of tetracycline (a) before 5 μg mL^{-1} and (b) after of removal.

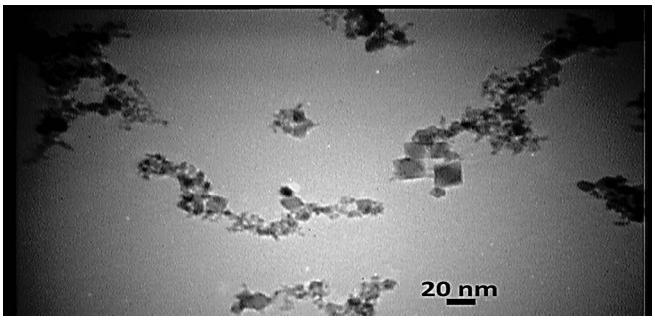

Fig. 3. TEM image of CeO_2 NPs.

3.2. TC adsorption studies

Fig. 5 shows the FT-IR spectra of the CeO_2 NPs, TC and the TC adsorbed CeO_2 NPs. The broad peak that is positioned at 3,400 cm^{-1} in all spectra is related to the OH group of the adsorbed water molecules. Also, the adsorption peaks around 1,630 cm^{-1} refer to the stretching vibration of the water bonds. In the FT-IR spectrum of the CeO_2 NPs

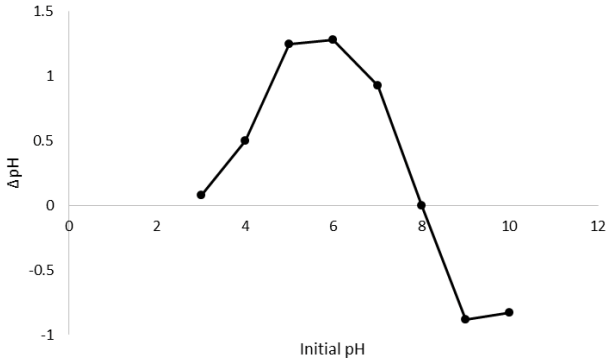

Fig. 4. PZC of adsorbent.

(Fig 5(a)), the peak that is centred at 495.34 cm^{-1} can be attributed to the Ce=O stretching vibration. The vibrational peaks observed from 1,000 to 1,350 cm^{-1} are consistent with those of commercial cerium oxide NPs. In the case of TC (Fig 5(b)), the 2,927.9 cm^{-1} peak is associated with the NHR^{3+} group and the peaks observed at 1,632.8 and 1,596.7 cm^{-1} are attributed to the C=O groups of the A and C rings (Fig. 1), respectively. In addition, the 1,744.3 and 1,521.3 cm^{-1} peaks can be ascribed to the amide group of TC. On the other hand, the FT-IR spectra of the TC-adsorbed NPs (Fig 5(c)) unravels a peak around 495.34 cm^{-1} that is related to the stretching vibration of Ce=O and the 1,598.7 and 1,541.4 cm^{-1} peaks corresponding to the C=O stretching vibration of TC. Therefore, it can be stated that TC is adsorbed onto the surface of the CeO_2 NPs. Furthermore, Fig. 5(c) indicates that the peaks related to the stretching modes of the polar TC groups are shifted toward shorter frequencies due to the adsorption of the TC polar groups onto the CeO_2 NPs. Accordingly, the C=O groups of TC should be adsorbed onto the positive surface of the CeO_2 NPs via H-bonding and the other polar groups of the TC molecules should be attracted to the CeO_2 NPs through electrostatic interactions [28]. The chemical reactions occurring between the CeO_2 NPs and the TC molecules are not known. However, according to similar

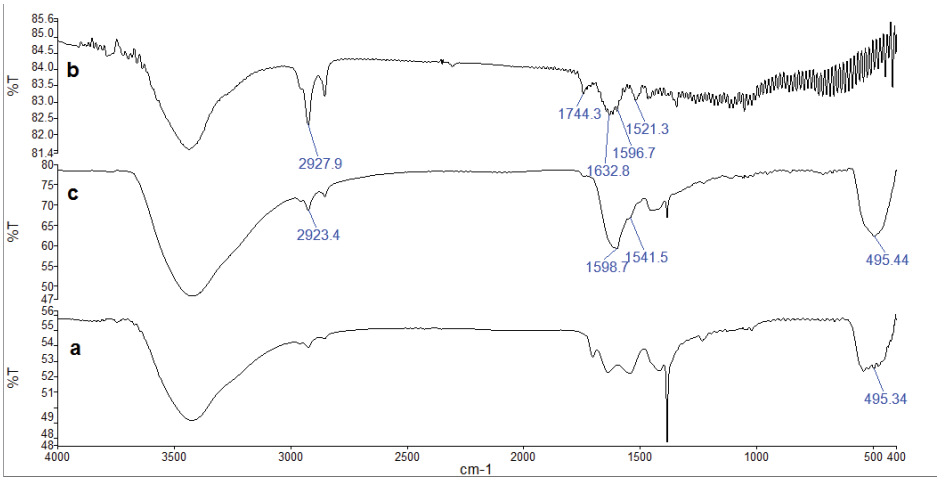

Fig. 5. The FT-IR spectra of (a) CeO_2 NPs, (b) TC, and (c) adsorbed TC on CeO_2 NPs.

adsorption systems, the mechanism might be controlled by diffusion processes due to the presence of electrostatic and H-bonding interactions between the surface of the adsorbent NPs and the polar functional groups of TC including its trimethylamine, amide, carbonyl, and phenolic groups. These interactions are possible through the nonbonded electron pairs of the oxygen and nitrogen atoms of TC or the π electrons associated with the TC rings [29].

3.3. Effect of pH

The pH of the sample solutions containing 5 mg L^{-1} TC was adjusted at 3–10 by adding HCl and/or NaOH (0.1 M) to evaluate the effect of pH on TC removal. The results are presented in Fig. 6. As this figure illustrates, pH has a significant impact on removal of TC. So that, increasing pH first enhances the efficiency of TC removal by the CeO_2 NPs and after a specific pH level decreases the efficiency. In this respect, changing pH from 5 to 8 alters the percentage of TC removal from 93.26% to 91.16% and identifies pH 7 as the optimal pH. As aforementioned, the PZC value of the CeO_2 NPs is 8 (Fig. 4). Therefore, the surface charge of the CeO_2 NPs is positive at pH levels below 8 and negative at pH values above 8. On the other hand, TC has multiple ionizable functional groups at pH < 3.0. In fact, TC is cationic at 3.0 < pH < 5.3, zwitterionic at 5.3 < pH < 6.3, and anionic at pH > 6.3 [1]. When pH of the solutions is in the range of 5–7, the TC molecules are negatively charged while the surface charge of the CeO_2 NPs is positive. Consequently, hence at pH 7 electrostatic attraction between the TC molecules and the surface of the CeO_2 NPs leads to an enhancement in the removal efficiency of TC. Since TC was removed effectively without adjusting the pH level of the solutions and to prevent pollution of the environment, pH of the TC solutions was not adjusted in further steps of this study.

3.4. Effect of the amount of CeO_2 NPs

Different amounts of the CeO_2 NPs (5–30 mg) were weighted and loaded into an extraction column with 10 cm length. The TC solutions were passed through the column at the flow rate of 1.3 mL min^{-1} at adjusted by a vacuum pump. Then, 20 μL of the output solution was injected into the HPLC system to determine its TC content and calculate the percentage of TC removal Fig. 7 displays the obtained results.

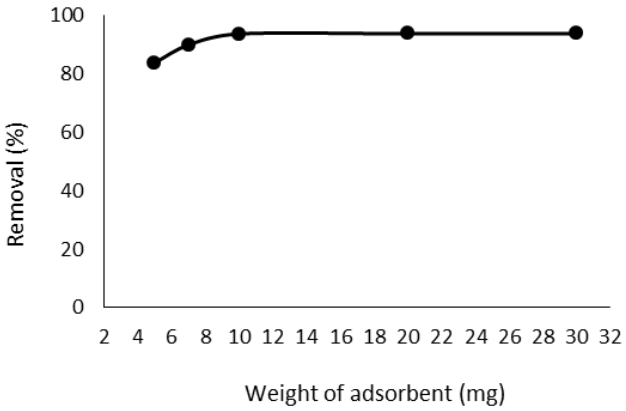

Fig. 7. Effect of adsorbent amount.

As it can be seen, applying 5 mg of the adsorbent results in 83.92% TC removal while the increase of the adsorbent amount to 10 mg promotes the removal efficiency to 93.80% due to the increased number of active sites for adsorption of the TC molecules onto the surface of the NPs. However, the percentage of TC removal remains constant by any further increase in the amount of the adsorbent. Therefore, 10 mg was selected as the optimal adsorbent amount.

3.5. Effect of sample solution flow rate

Several sample solutions with the same TC concentration were passed through the column at different flow rates. The corresponding results are exhibited in Fig. 8. With respect to this figure, the flow rate of 2.5 mL min^{-1} gives 72.77% TC removal. This extent of TC adsorption increases by reducing the rate of sample flow through the adsorbent column and reaches to 93.83% using the 1.3 mL min^{-1} flow rate. In other words, adsorption of TC onto the adsorbent improves due to the increased time of contact between the sample working and the adsorbent. Accordingly, the 1.3 mL min^{-1} flow rate was chosen as the optimal rate of solution flow.

3.6. Effect of ionic strength

The effect of ionic strength was evaluated at different concentrations of the NaCl electrolyte. Fig. 9 shows the related removal efficiencies. Based on this figure, the highest

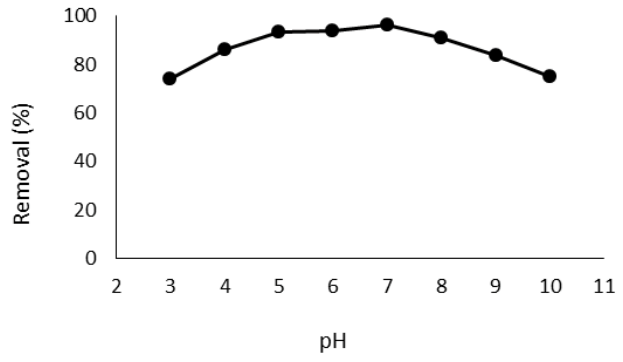

Fig. 6. Effect of pH.

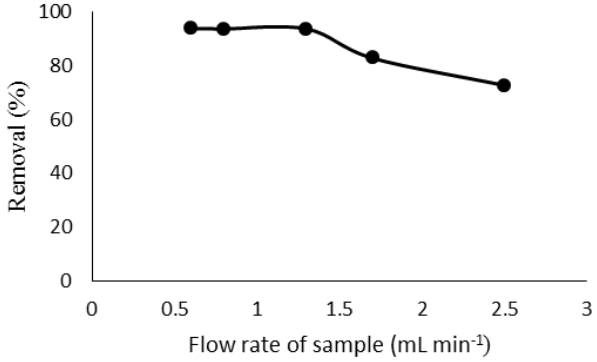

Fig. 8. Effect of sample solution flow rate.

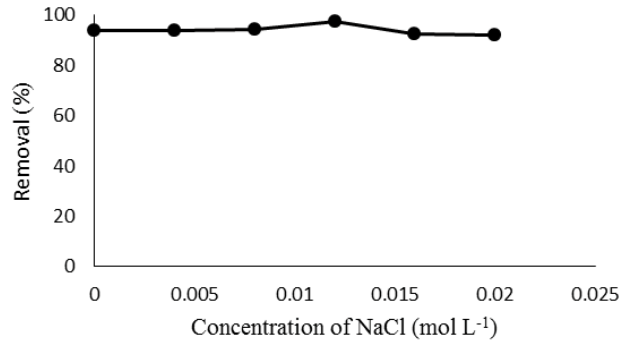

Fig. 9. Effect of ionic strength.

percentage of TC removal, that is, > 97.58%, is obtained at the 0.012 M electrolyte concentration and the efficiency of TC removal decreases gradually with the decrease of electrolyte concentration. This result implies that electrostatic interactions play a significant role in adsorption of TC. Since the fact that the overall change in the percentage of TC removal is not significant, no electrolyte should be added to the adsorption system for the sake of environmental protection. Therefore, it can be concluded that electrostatic interactions did play significant role in adsorption of TC.

3.7. Effect of sample volume

The effect of the initial sample volume on TC removal was investigated using a series of solutions with a fixed amount of TC (125 μg) added to 25, 50, 100, and 150 mL distilled water. In the case of the 10 mL sample, the efficiency of TC removal was 95.26% and TC adsorption onto the surface of the adsorbent did not decrease significantly by increasing the volume of the solution up to 100 mL. For the 100 mL volume, the percentage of TC removal was 89.82% while the use of 150 mL sample volume declined the efficiency of TC removal, due to the solution dilution and desorption of the TC molecules from the adsorbent's surface. Therefore, the maximum tolerable volume of the solution is 100 mL (see Fig. 10).

3.8. Adsorption isotherms

Several isotherm models, such as the Langmuir and Freundlich isotherms, have been used to study the isotherms of various adsorption systems by different researchers [30].

Similarly, in this study, the Langmuir and Freundlich models were used to determine the ability of the CeO_2 NPs in adsorbing TC from aqueous solutions. For this purpose, TC removal in batch mode was monitored for 40 min and the adsorption system was found to equilibrate within 20 min. Eqs. (1) and (2) are the mathematical expressions of the Langmuir and Freundlich models, respectively.

$$\frac{C_e}{q_e} = \frac{C_e}{q_{\max}} + \frac{1}{q_{\max} K_L} \tag{1}$$

$$\log q_e = \log K_F + \frac{1}{n} \log C_e \tag{2}$$

In these equations C_e is equilibrium density (μg mL^{-1}), q_e is the amount of TC adsorbed at equilibrium (mg g^{-1}), $q_{\max}$ is the maximum capacity of the adsorbent (mg g^{-1}), and K_L and K_F are the adsorption equilibrium constants of the two models (L mg^{-1}) [31]. After calculating the concentration of the effluent solutions at the equilibrium time, the amount of the TC molecules adsorbed onto the NPs at time t, that is, q_t (mg L^{-1}), was calculated through Eq. (3) as follows [31]:

$$q_t = \left(C_i - C_t\right) \times \frac{V}{W} \tag{3}$$

where C_i (mg L^{-1}) is the initial TC concentration, C_t (mg L^{-1}) is TC concentration at time t, V (L) is the volume of the solution, and W (g) is the mass of the NPs. It should be noted that the q_e, C_e, q_t, and C_t variables refer to the equilibrium status. According to the Langmuir and Freundlich isotherm curves presented in Fig. 11, the maximum capacity of the CeO_2 NPs for adsorption of TC is 74.03 mg g^{-1}. Furthermore, based on the results of the two isotherm models (Table 2), correlation coefficient for Langmuir isotherm is greater than that of the Freundlich isotherm. Therefore, adsorption of TC onto the CeO_2 NPs follows the Langmuir isotherm. With respect to this isotherm [Eq. (1)], the maximum capacity of the CeO_2 NPs for adsorption of TC is 79.36 mg g^{-1} and the K_L value equals to 0.594 L mg^{-1}.

3.9. Adsorption kinetics

Several kinetics models have been suggested for description of adsorption processes. In this study, the pseudo-first-order

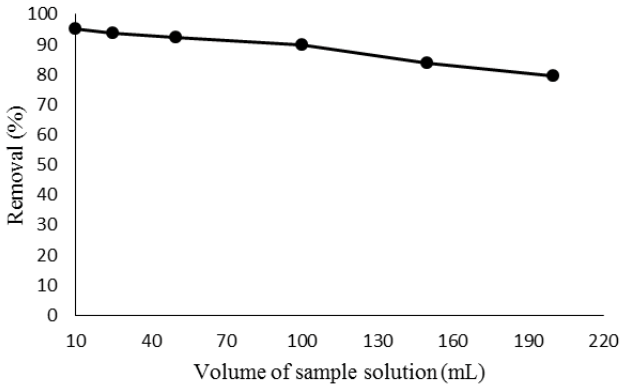

Fig. 10. Effect of sample volume.

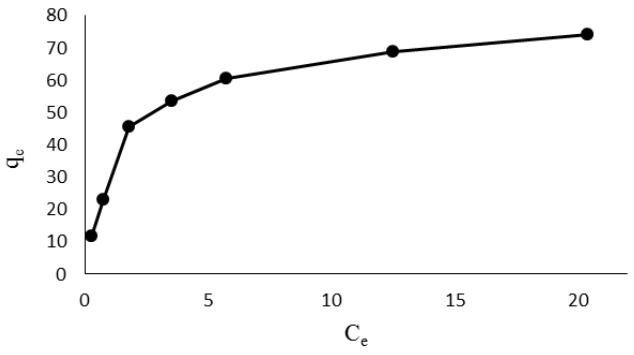

Fig. 11. Isotherm curve.

Table 2
Data of adsorption isotherms

Langmuir			
Equation	q_{max} (mg g^{-1})	K_L (L mg^{-1})	R
$y = 0.0126x + 0.0212$	79.365	0.594	0.9994
Freundlich			
Equation	K_F (mg g^{-1})	N	R
$y = 0.4205x + 1.4179$	26.175	2.378	0.9494

model suggested by Lagergren and the pseudo-second-order model were adopted. The logarithmic equations of these models at boundary conditions ($t = 0$ to $t = t$ and $q = 0$ to $q = q$) follow Eqs. (4) and (5), respectively [32].

$$\log\left(q_e - q_t\right) = \log q_e - \frac{K_1 t}{2.303} \tag{4}$$

$$\frac{t}{q_t} = \frac{1}{K_2 q_e^2} + \frac{t}{q_e} \tag{5}$$

For the second- and first-order models, log (q_e–q_t) versus t [Eq. (4)] and t/q_t versus t [Eq. (5)] should be respectively plotted to determine the kinetic parameters [32]. The corresponding plots were applied to the data obtained by using 5 and 10 μg mL^{-1} TC in a batch experiment for 20 min. According to the results (Table 3), the correlation coefficients for the pseudo-second-order model are closer to the unity relative to those of the pseudo-first-order model. Therefore, the TC adsorption process follows the pseudo-second-order kinetic model.

3.10. Effect of coexisting ions

To study applicability of the adsorption system to solutions with different matrices, the effect of several ions and antibiotics on TC removal under the optimum conditions was evaluated. The maximum acceptable measurement error was ±5%. The results are reported in Table 4.

Table 5
Real sample analysis

Real sample	Added (μg mL^{-1})	Removal %
Dez river water	0	—
	5	93.04
Drinking water	0	—
	5	93.59

3.11. Analysis of real sample

To investigate the ability of the adsorption system in removing TC from a real TC containing matrix, spiked samples were used. The examined solutions were sampled from the Dez River (Ahvaz, Iran) and the tap water of the Ahvaz town (Khozestan, Iran). According to the results (Table 5), the CeO_2 NPs can provide satisfactory removal percentages, which means that the matrix components of the water samples do not interfere with the main adsorption reaction.

4. Conclusions

The findings of this study demonstrated that the proposed adsorption method can be successfully and effectively used for removal of the TC antibiotic from aqueous samples. The developed method is simple, clean, fast, and low-cost and requires a low amount of adsorbent. According to the results of the isotherm experiment, adsorption of TC onto the CeO_2 NPs follows the Langmuir isotherm. The adsorption capacity of the cerium oxide nanoparticles for TC was found to be 79.365 mg g^{-1}. Moreover, the results showed that ionic

Table 3
Kinetic parameters

	Concentration (μg mL^{-1})	Equation	R	
				K_1 (min^{-1})
Pseudo-first-order model	5	$y = –0.0613x + 0.6421$	0.9725	0.141
	10	$y = –0.0828x + 1.1923$	0.9736	0.191
				K_2 (g mg^{-1} min^{-1})
Pseudo-second-order model	5	$y = 0.0819x + 0.1167$	0.9987	0.057
	10	$y = 0.0392x + 0.0942$	0.9980	0.016

Table 4
Interference effects on removal of TC

Species	Tolerance ratio
Zn^{2+}	7
Ni^{2+}	8
F^-, NH_4^+	25
Cd^{2+}	40
Mn^{2+}, K^+, SCN^-	> 100
Pencillin G, Amoxicillin, Ampicillin, Chlorotetracycline	Was interfere up one equal of concentration

strength has an insignificant effect on removal efficiency and kinetics of the adsorption process obeys the pseudo-second-order model. Adsorption of TC onto the cerium oxide nanoparticles is driven by electrostatic interactions and formation of hydrogen bonds between the functional groups of TC and cerium oxide nanoparticles.

Acknowledgment

The authors wish to thank Shahid Chamran University of Ahvaz for financial support of this project (grant 1396).

References

[1] Q. Liu, Y. Zheng, L. Zhong, X. Cheng, Removal of tetracycline from aqueous solution by a Fe_3O_4 incorporated PAN electrospun nanofiber mat, J. Environ. Sci., 28 (2015) 29–36.
[2] H. Liu, Y. Yang, J. Kang, M. Fan, J. Qu, Removal of tetracycline from water by Fe-Mn binary oxide, J. Environ. Sci., 24 (2012) 242–247.
[3] L. Wang, H. Yang, C. Zhang, Y. Mo, X. Lu, Determination of oxytetracycline, tetracycline and chloramphenicol antibiotics in animal feeds using subcritical water extraction and high performance liquid chromatography, Anal. Chem. Acta, 619 (2008) 54–58.
[4] I. Chopra, M. Roberts, Tetracycline antibiotics: mode of action, applications, molecular biology, and epidemiology of bacterial resistance, Microbiol. Mol. Biol. Rev., 65 (2001) 232–260.
[5] R.S. Valverde, I.S.A. Pérez, F. Franceschelli, Determination of photoirradiated tetracyclines in water by high-performance liquid chromatography with chemiluminescence detection based reaction of rhodamine B with cerium (IV), J. Chromatogr. A., 1167 (2007) 85–94.
[6] Z. Zhang, H. Lan, H. Liu, J. Qu, Removal of tetracycline antibiotics from aqueous solution by amino-Fe (III) functionalized SBA15, Colloid Surf. A: Physicochem. Eng. Aspects, 471 (2015) 133–138.
[7] S. Li, T. Mei, Y. Peng, S. Ge, G. Wang, Y. Zhu, L. Ni, Y. Zhang, Rapid removal of tetracycline (TC) by ozonation after extraction TC from water into acetic acid solution using granular activated carbon, Sci. Eng., 37 (2015) 405–410.
[8] L. Xu, Y. Sun, L. Du, J. Zhang, Removal of tetracycline hydrochloride from wastewater by nanofiltration enhanced by electro-catalytic oxidation, Desalination, 352 (2014) 58–65.
[9] G. Safari, M. Hoseini, H. Kamali, R. Moradirad, A. Mahvi, Photocatalytic degradation of tetracycline antibiotic from aqueous solutions using UV/TiO_2 and UV/H_2O_2/TiO_2, J. Health, 5 (2014) 203–2013.
[10] G.H. Safari, M. Hoseini, M. Seyedsalehi, H. Kamani, J. Jaafari, A.H. Mahvi, Photocatalytic degradation of tetracycline using nanosized titanium dioxide in aqueous solutio, J. Environ. Sci., 12 (2015) 603–616.
[11] D. Belkheiri, F. Fourcade, F. Geneste, D. Floner, H. Aït-Amar, A. Amrane, Combined process for removal of tetracycline antibiotic – coupling pre-treatment with a nickel-modified graphite felt electrode and a biological treatment, Intern. Biodet. Biodeg., 103 (2015) 147–153.
[12] Y. Lin, S. Xu, J. Li, Fast and highly efficient tetracyclines removal from environmental waters by graphene oxide functionalized magnetic particles, Chem. Eng. J., 225 (2013) 679–685.
[13] Y. Gao, Y. Li, L. Zhang, H. Huang, J. Hu, S.M. Shah, X. Su, Adsorption and removal of tetracycline antibiotics from aqueous solution by graphene oxide, J. Colloid Interface Sci., 368 (2012) 540–546.
[14] P.-H. Chang, Z. Li, T.-L. Yu, S. Munkhbayer, T.-H. Kuo, Y.-C. Hung, J.-S. Jean, K.-H. Lin, Sorptive removal of tetracycline from water by palygorskite, J. Hazard. Mater., 165 (2009) 148–155.
[15] S.A. Sassman, L.S. Lee, Sorption of three tetracyclines by several soils: assessing the role of pH and cation exchange, J. Environ. Sci., Technol., 39 (2005) 7452–7459.
[16] H.R. Pouretedal, N. Sadegh, Effective removal of Amoxicillin, Cephalexin, Tetracycline and penicillin G from aqueous solutions using activated carbon nanoparticles prepared from vine wood, Water Eng. Proc., 1 (2014) 64–73.
[17] X. Rong Jing, Y. Ying Wang, W. Jung Liu, Y. Kun Wang, H. Jiang, Enhanced adsorption performance of tetracycline in aqueous solutions by methanol-modified biochar, Chem. Eng. J., 248 (2014) 168–174.
[18] S.B. Kabakc, A. Thompson, E. Cartmell, K. Le Corre, Adsorption and precipitation of tetracycline with struvite, J. Water Environ. Fed., 79 (2007) 2551–2556.
[19] G. Moussavi, A.M. Salehi, K. Yaghmaeian, The catalytic destruction of antibiotic tetracycline by sulfur-doped manganese oxide (SeMgO) nanoparticles, J. Environ. Manage., 210 (2018) 131–138.
[20] W. Ru Chen, C. Hua Huang, Adsorption and transformation of tetracycline antibiotics with aluminum oxide, Chemospher, 79 (2010) 779–785.
[21] O. Hanay, B. Yıldız, S. Aslan, H. Hasar, Removal of tetracycline and oxytetracycline by microscale zerovalent iron and formation of transformation products, Environ. Pollut., 21 (2014) 3774–3782.
[22] S. Liu, P. Wu, L. Yu, L. Li, B. Gong, N. Zhu, Z. Dang, C. Yang, Preparation and characterization of organo-vermiculite based on phosphatidylcholine and adsorption of two typical antibiotics, Appl. Clay Sci., 137 (2017) 160–167.
[23] Y. Zhao, J. Geng, X. Wang, X. Gu, S. Gao, Tetracycline adsorption on kaolinite: pH, metal cations and humic acid effects, Ecotoxicology, 20 (2011) 1141–1147.
[24] K.R. Alhooshani, Adsorption of chlorinated organic compounds from water with cerium oxide-activated carbon composite, Arab. J. Chem., 15 (2015) 115–139.
[25] Y. Li, P. Li, H. Yu, Y. Bian, Recent advances (2010–2015) in studies of cerium oxide nanoparticles' health effects, Environ. Toxicol. Phar., 44 (2016) 25–29.
[26] R. Li, Q. Li, S. Gao, J.K. Shang, Exceptional arsenic adsorption performance of hydrous cerium oxide nanoparticles: part A. Adsorption capacity and mechanism, Chem. Eng. J., 185 (2012) 127–135.
[27] J. Wang, W. Xu, L. Chen, Y. Jia, L. Wang, X. Huang, J. Liu, Excellent fluoride removal performance by CeO_2–ZrO_2 nanocages in water environment, Chem. Eng. J., 231 (2013) 198–205.
[28] M. Brigante, P.C. Schulz, Cerium (IV) oxide: synthesis in alkaline and acidic media, characterization and adsorption properties, Chem. Eng. J., 191 (2012) 563–570.
[29] M. Brigante, P. Schulz, Adsorption of the antibiotic minocycline on cerium(IV) oxide: effect of pH, ionic strength and temperature, Micro. Meso. Mat., 156 (2012) 138–144.
[30] K.Y. Foo, B.H. Hameed, Insights into the modeling of adsorption isotherm systems, Chem. Eng. J., 156 (2010) 2–10.
[31] A.A. Inyinbor, F.A. Adekola, G.A. Olatunji, Kinetics, isotherms and thermodynamic modeling of liquid phase adsorption of Rhodamine B dye onto *Raphia hookerie* fruit epicarp, Wat. Resour. Educ., 15 (2016) 14–27.
[32] S. Azizian, Kinetic models of sorption: a theoretical analysis, J. Colloid Interface Sci., 276 (2004) 47–52.